NASA TECHNICAL NOTE

NASA TN D-6426

NASA TN D-6426

THE ELASTIC RESPONSE OF BIAS-PLY AIRCRAFT TIRES TO BRAKING FORCES

by John A. Tanner, John L. McCarty, and Sidney A. Batterson

Langley Research Center
Hampton, Va. 23365

NATIONAL AERONAUTICS AND SPACE ADMINISTRATION • WASHINGTON, D. C. • SEPTEMBER 1971

1. Report No. NASA TN D-6426	2. Government Accession No.	3. Recipient's Catalog No.
4. Title and Subtitle THE ELASTIC RESPONSE OF BIAS-PLY AIRCRAFT TIRES TO BRAKING FORCES		5. Report Date September 1971
		6. Performing Organization Code
7. Author(s) John A. Tanner, John L. McCarty, and Sidney A. Batterson		8. Performing Organization Report No. L-6605
		10. Work Unit No. 133-61-12-01
9. Performing Organization Name and Address NASA Langley Research Center Hampton, Va. 23365		11. Contract or Grant No.
		13. Type of Report and Period Covered Technical Note
12. Sponsoring Agency Name and Address National Aeronautics and Space Administration Washington, D.C. 20546		14. Sponsoring Agency Code
15. Supplementary Notes		

16. Abstract

A study was made to evaluate the elastic behavior of a braked rolling tire and to relate this behavior to the tire characteristics obtained from simple static flexure tests. The study consisted of static and braked-rolling tests of two types of bias-ply aircraft tires and an analysis which related tire reaction to the braking forces.

The results of this investigation indicate that the elastic response of an aircraft tire to braking forces can be defined by the displacement distribution along the tire periphery and by the fore-and-aft spring constant. Changes in the rolling radius due to braking can be predicted with reasonable accuracy from elastic measurements of the static free-tread periphery or from elastic measurements within the footprint during low-speed braking, assuming there is no slippage between the tire and the pavement. The results of these tests further indicate that what was heretofore considered as pure tire slippage under braked-rolling conditions may be wholly or in part the result of tire elasticity. The elasticity must be considered in the design or application of efficient automatic braking systems.

17. Key Words (Suggested by Author(s)) Aircraft tires, Elasticity, Braking performance		18. Distribution Statement Unclassified – Unlimited	
19. Security Classif. (of this report) Unclassified	20. Security Classif. (of this page) Unclassified	21. No. of Pages 30	22. Price* $3.00

*For sale by the National Technical Information Service, Springfield, Virginia 22151

THE ELASTIC RESPONSE OF BIAS-PLY AIRCRAFT TIRES TO BRAKING FORCES

By John A. Tanner, John L. McCarty,
and Sidney A. Batterson
Langley Research Center

SUMMARY

A study was made at Langley Research Center to evaluate the elastic behavior of a braked rolling tire and to relate this behavior to the tire characteristics obtained from simple static flexure tests. The study consisted of static and braked-rolling tests of two types of bias-ply aircraft tires and an analysis which related tire reaction to the braking forces.

The results of this investigation indicate that the elastic response of an aircraft tire to braking forces can be defined by the displacement distribution along the tire periphery and by the fore-and-aft spring constant. Changes in the rolling radius due to braking can be predicted with reasonable accuracy from elastic measurements of the static free-tread periphery or from elastic measurements within the footprint during low-speed braking, assuming there is no slippage between the tire and the pavement. The results of these tests further indicate that what was heretofore considered as pure tire slippage under braked-rolling conditions may be wholly or in part the result of tire elasticity. The elasticity must be considered in the design or application of efficient automatic braking systems.

INTRODUCTION

Many of the aircraft ground handling problems can be traced to a lack of understanding of the elastic behavior of the pneumatic tire. The shortage of meaningful data on the static and dynamic properties of tires impedes the solution of problems associated with airplane braking performance, landing-gear shimmy, steering, bogie pitching, etc., and results in considerable delays and costs to the manufacturer. Such information, particularly with respect to the lateral and fore-and-aft elastic tire behavior, would permit the development of rational methods for analyzing the dynamic response of a landing-gear system. Some experimental and analytical data exist on the lateral deformation of an aircraft tire under both static loading and low-speed yawed-rolling conditions (refs. 1 to 4) for use in landing-gear-shimmy analyses. However, data on the fore-and-aft elastic properties of tires are limited to static experimental tests (refs. 5 to 8) and an empirical analysis (ref. 9) which was based upon the tire stretch distribution as presented in reference 8. No data exist which describe the elastic response of tires under braked-rolling conditions.

A knowledge of the tire response in the fore-and-aft direction is important for safer and more economical operations of the automatic braking systems employed by most present-day commercial and military aircraft. In their operation, these systems control the application of brake torque by sensing wheel angular acceleration. However, because of the elastic nature of the tire, the angular acceleration of the wheel can significantly differ from that of the tire, particularly at the tire-pavement interface where the braking traction is developed. This spring coupling between the brake and the pavement governs the operational behavior of the braking system and, as pointed out in reference 10, is not fully understood. Furthermore, current tire procurement specifications ignore the elastic properties of a tire although it has been observed that tires of the same size but from different manufacturers have dissimilar elastic characteristics. This neglect can result in significant differences in the operational performance of a braking system which is reflected in the stopping distance and the directional-control capabilities of the aircraft. Thus a need exists to define the elastic behavior of a tire undergoing braking in order to develop more meaningful tire specifications and to aid in designing more efficient automatic braking systems.

The objective of this paper is to present the results of a study to evaluate the elastic behavior of a braked rolling tire and to relate this behavior to the tire characteristics obtained from static flexure tests. The study consisted of static and rolling tests of two types of bias-ply aircraft tires and an analysis which related tire reaction to the braking forces. The experimental tests were conducted at the Langley landing-loads track at ground speeds up to 100 knots.

SYMBOLS

Values are given in both SI and U.S. Customary Units. The measurements and calculations were made in U.S. Customary Units.

e	base of natural logarithms
F_x	braking force, kN (lb)
F_z	vertical load, kN (lb)
J_x	decay length, cm (in.)

K_x static fore-and-aft spring constant, kN/cm (lb/in.)

r unloaded, inflated tire radius, cm (in.)

r_e braked tire rolling radius, cm (in.)

r_o unbraked tire rolling radius, cm (in.)

Δr change in rolling radius resulting from braking forces, cm (in.)

s circumferential distance, cm (in.)

u displacement, cm (in.)

ϵ_x elongation strain due to braking force

ϵ_z elongation strain due to vertical load

Subscripts:

calc calculated

exp experimental

f leading half of footprint

max maximum

p free-tread periphery

p_i peripheral station

p_o footprint leading edge

APPROACH

The elastic properties of a braked rolling tire are primarily reflected in the tire rolling radius. The rolling radius of a tire is defined as the ratio of the horizontal displacement of the wheel axle to the angular displacement of the wheel and is a variable quantity which, in the unyawed case, is influenced primarily by the tire vertical load and the longitudinal force on the tire due to braking (braking force). The braking-force contribution to changes in the rolling radius of a tire under a constant vertical load is the direct result of tire stretch or elasticity. The empirical analysis of reference 9 relates the tire rolling radius to tire elasticity through the fore-and-aft tire spring constant and the variation in the deformation within the free-tread periphery of the tire (see fig. 1) as determined from several static-loading tests. The analysis of reference 9 was based upon the assumptions that limited peripheral measurements in the free tread adequately described the tire deformation while undergoing braking and, further, that the tire footprint deformed as a unit, i.e., with no localized stretching within the footprint. The

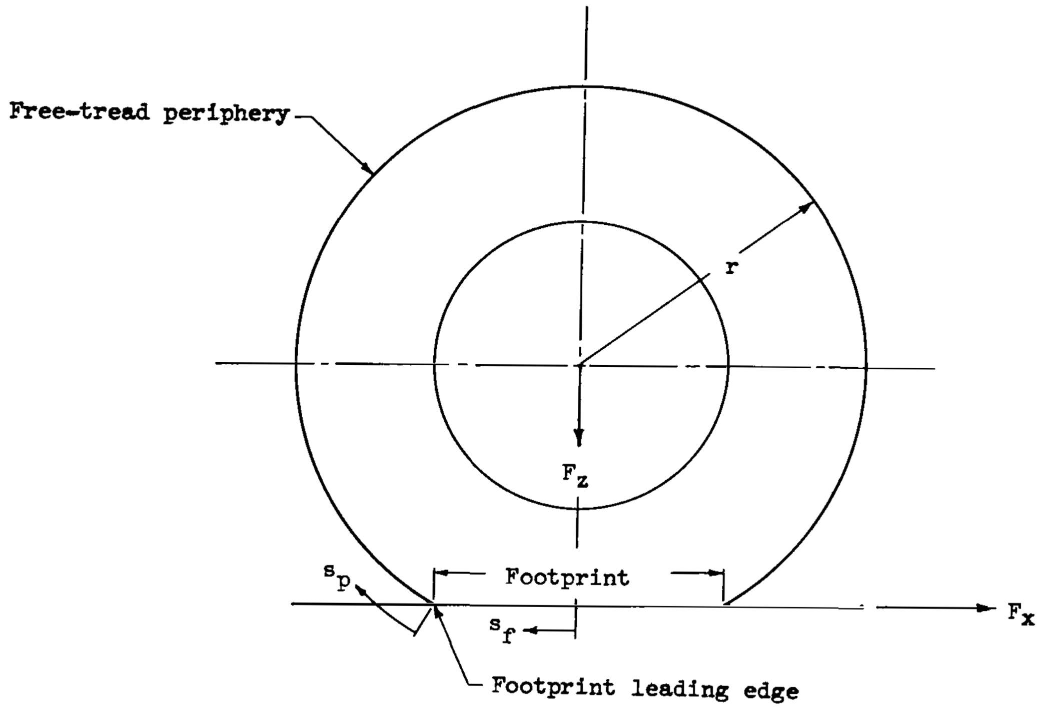

(a) Tire nomenclature.

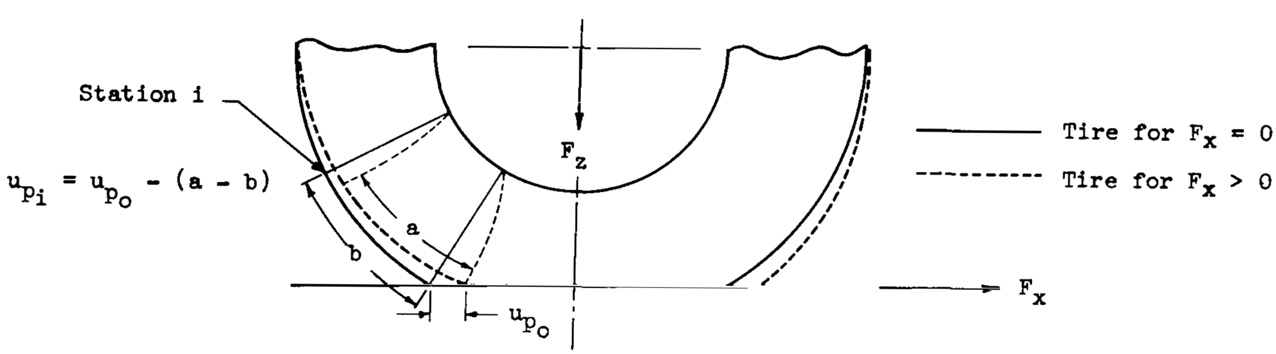

(b) Deformation in free-tread periphery.

Figure 1.- Sketches illustrating tire nomenclature and deformation in free-tread periphery under combined vertical load and braking force.

purpose of this investigation was to study the fore-and-aft elastic, or braking properties of two types of tires under both static-loading and braked- and unbraked-rolling conditions in an attempt to: (1) evaluate the assumptions necessary for the analysis of reference 9, (2) establish an expression for the braked rolling radius based upon tire-stretch measurements within the footprint under braked-rolling conditions, and (3) compare the results from this expression and that of reference 9 with corresponding results from experimental braked- and unbraked-rolling tests.

The program undertaken to accomplish the goals of this study consisted of experimental tests both under static loadings (to simulate a braked wheel) and under actual braked- and unbraked-rolling conditions. The static tests provided measurements of the overall footprint displacement to determine each tire spring constant, and deformation within both the footprint and a selected region of the tire free-tread periphery. The results of these tests were used to validate the assumptions of reference 9. The braked- and unbraked-rolling tire tests were conducted to provide information inputs necessary to develop and evaluate an empirical analysis to predict the tire elastic response.

APPARATUS AND TEST PROCEDURE

Static-loading and braked- and unbraked-rolling tests were conducted on two types of high-pressure, high-speed bias-ply aircraft tires: a 30 × 11.5-14.5 type VIII tire with fabric and wire-reinforced tread (tire A); and a 49 × 17 type VII tire with a natural rubber recap tread (tire B). Figure 2 is a photograph of the two tires and table I lists their pertinent characteristics. Both the static-loading and rolling tests were conducted with the

TABLE I.- TIRE CHARACTERISTICS

	Tire A	Tire B
Tire size	30 × 11.5-14.5	49 × 17
Type	VIII	VII
Ply rating	26	26
Type of ply	Bias	Bias
Test inflation pressure, N/cm^2	145	117
(lb/in^2)	(210)	(170)
Unloaded, inflated radius, cm	37.45	61.8
(in.)	(14.73)	(24.34)
Rated maximum vertical load, kN	111	176
(lb)	(25 000)	(39 600)
Rated maximum speed, knots	210	190
Tread description	Natural rubber, fabric and wire reinforced rib tread	Natural rubber, recap rib tread

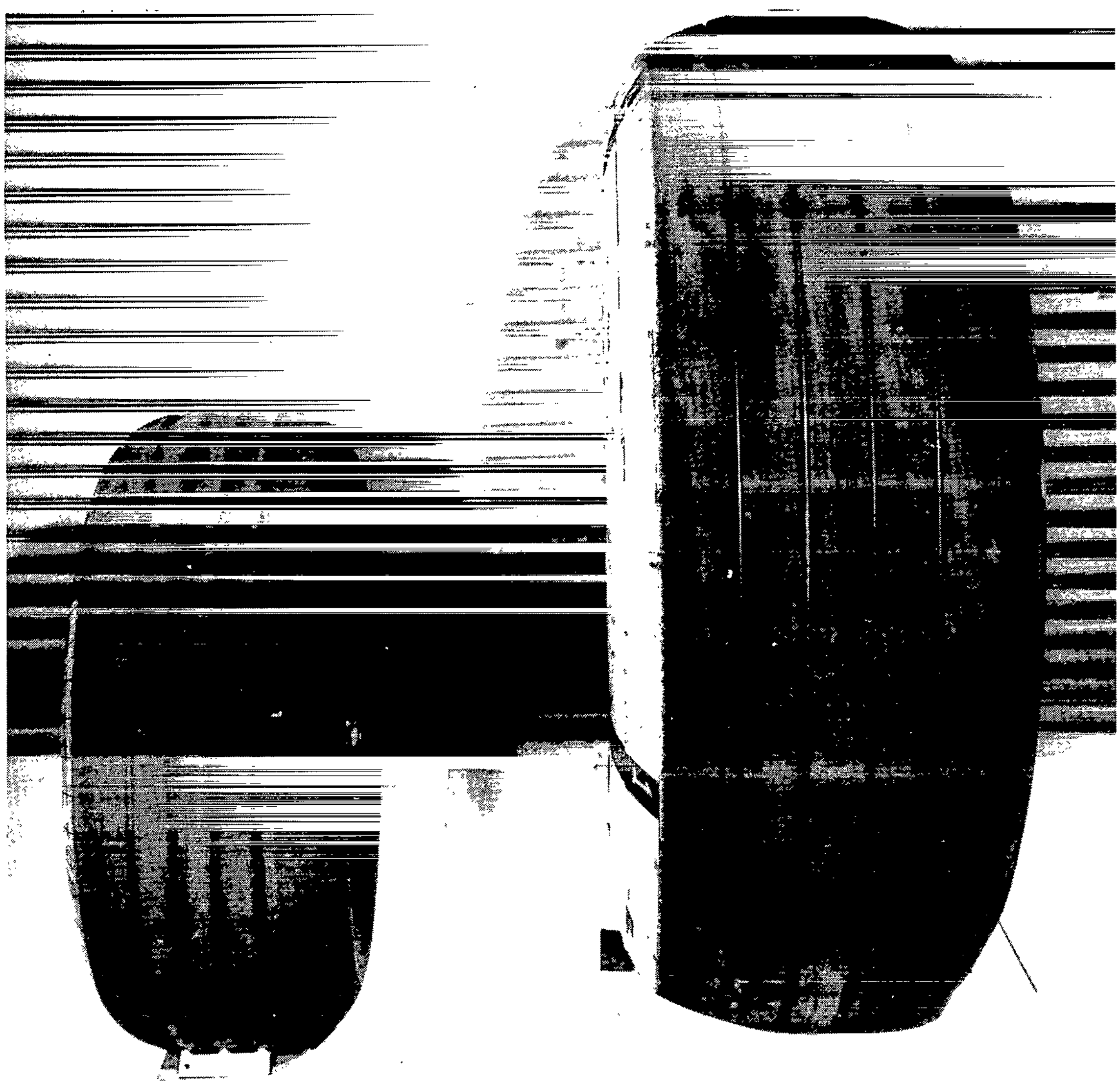

L-71-653

Figure 2.- Aircraft tires used in the investigation.

wheel, tire, and brake assembly mounted on the large carriage at the Langley landing-loads track. (See ref. 11.)

Static-Loading Tests

The objectives of the static-loading tests were to determine the fore-and-aft spring constants of the tires and to measure tire deformation or stretch along the free-tread periphery and within the footprint. Three different test procedures were required to meet these objectives and each is described separately in the paragraphs which follow.

Spring constants.- Figures 3 and 4 are photographs of the test equipment employed to determine the fore-and-aft spring constants of the test tires. This equipment consisted of the test tire which rested, under a vertical load, on the surface of a bearing plate and the instrumentation necessary to monitor the tire loadings and the bearing-plate displacements. The wheel was externally braced, as shown in figure 3, to prevent axle translation and wheel rotation. Tire loadings included the vertical load which was controlled by the carriage hydraulic system (refs. 11 and 12) and the fore-and-aft load, or braking force, which was applied to the bearing plate by means of the hydraulic piston identified in figure 3. The magnitude of the vertical load applied to the tire was measured by load cells under the bearing plate and the braking force was measured by a load cell located between the hydraulic piston and the backstop. The braking forces were restricted to levels insufficient to produce any discernible slippage in the tire—bearing-plate interface. Fore-and-aft displacements of the bearing plate during application of the braking force were obtained from a dial indicator graduated into thousandths of an inch. Since there was no relative motion (no slippage) between the tire footprint and the bearing plate, these bearing-plate displacements correspond to the footprint displacements.

The testing technique involved the application of the desired vertical load to the tire, the incremental application of a braking force, and the recording of the resulting displacements of the overall tire footprint. Spring constants were determined for tire A under nominal vertical loads of 51.2 and 98 kN (11 500 and 22 000 lb) and for tire B under nominal vertical loads of 107 and 138 kN (24 000 and 31 000 lb).

Deformation in free-tread periphery.- Deformations in the free-tread periphery were measured concurrent with the spring constants. In preparation for these measurements, a number of cone-shaped rubber studs were attached along the periphery of each tire as shown in figure 4 and a camera was mounted to a beam which was free to rotate about the axle center line. Free-tread peripheral deformations were obtained from enlarged photographs taken of the studs during the course of the static-loading tests.

Deformation within the footprint.- Deformation within the footprint resulting from combined vertical and braking forces on the tire was determined from photographs taken of the tire footprint through a glass plate installed in the test section of the landing-loads

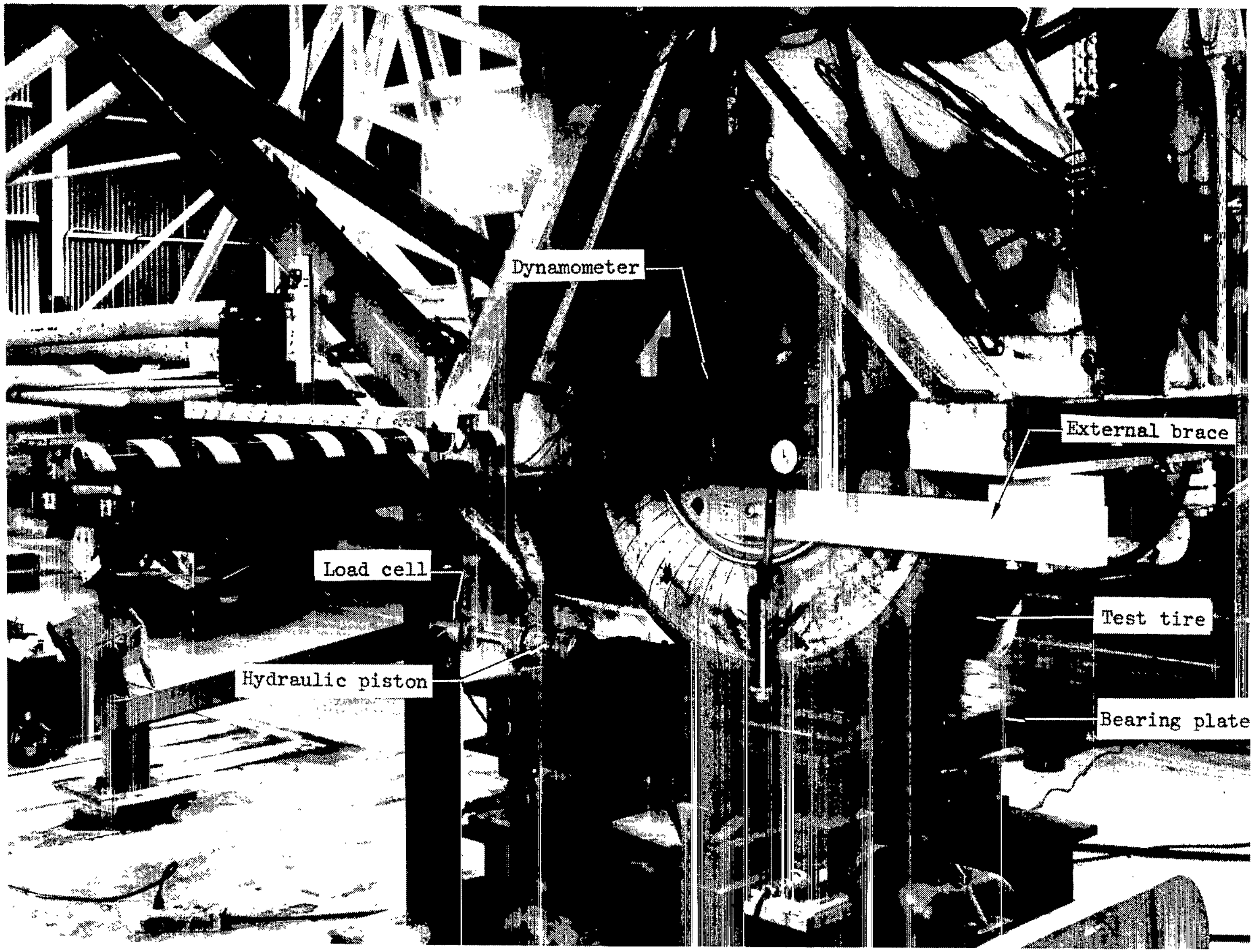

L-71-654

Figure 3.- Static-loading test equipment for evaluating tire fore-and-aft spring constant.

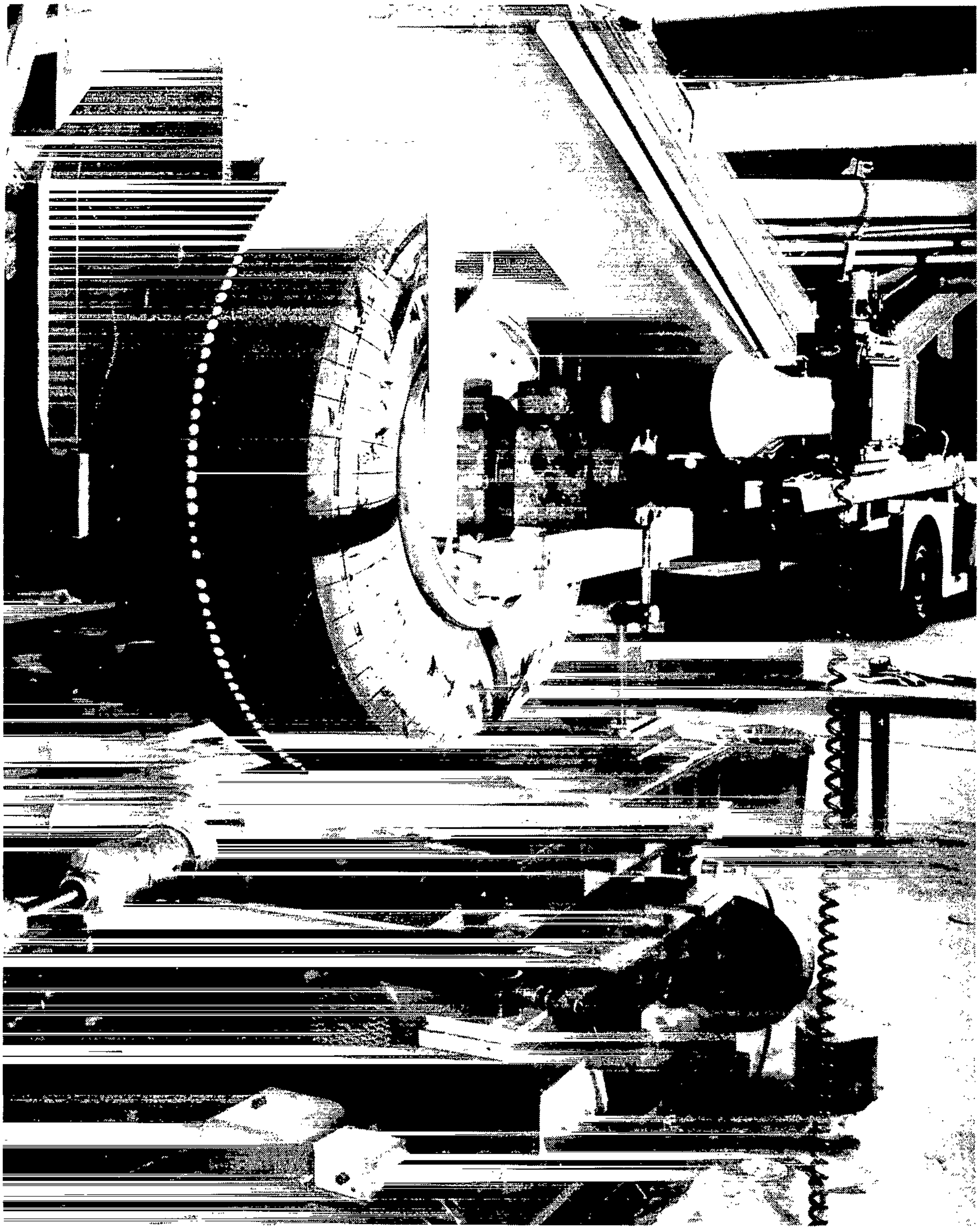

L-71-655

Figure 4.- Photograph of static-loading test equipment showing cone-shaped rubber studs for measuring deformations in tread periphery.

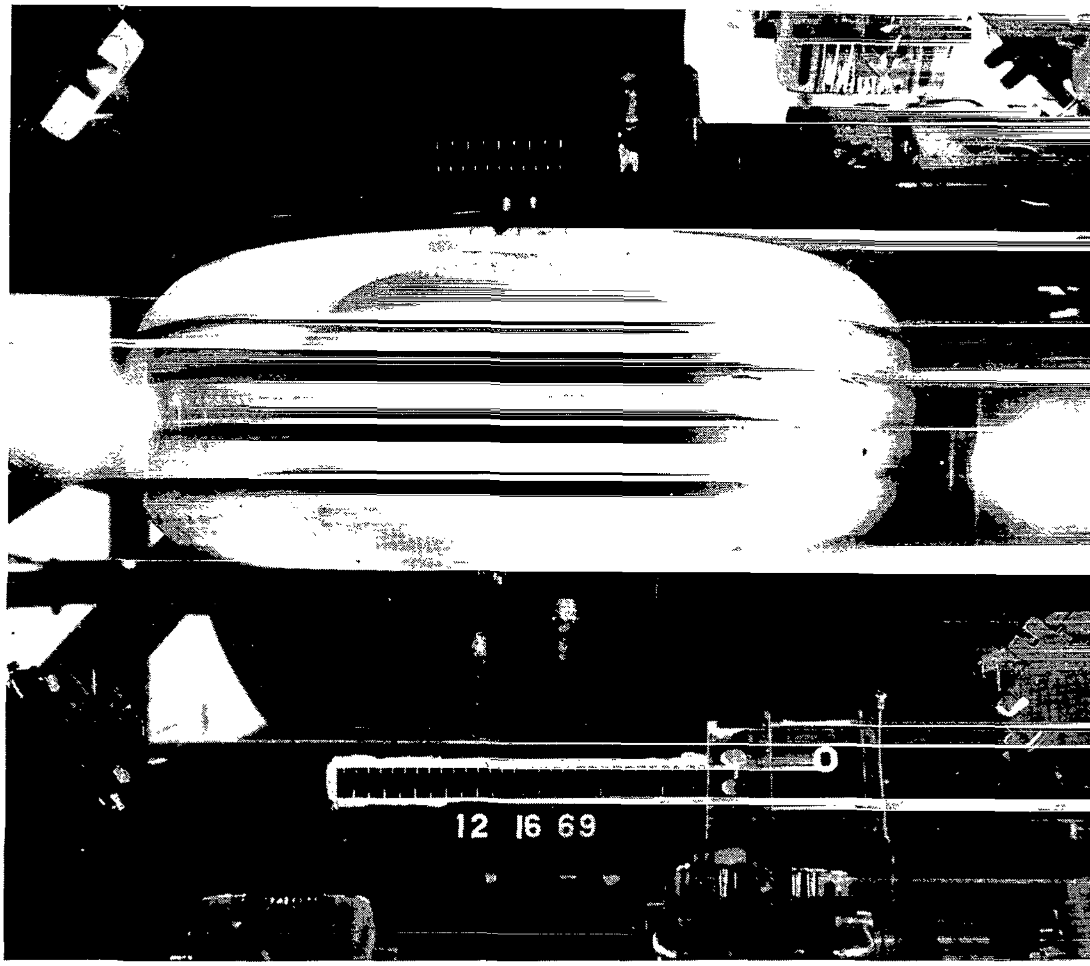

L-71-656

Figure 5.- Tire footprint as seen from beneath glass plate.

track. In preparation for these tests, equally spaced small holes 3.2 mm (1/8 in.) in diameter and 1.6 mm (1/16 in.) deep were drilled along the tire periphery and filled with white silicon rubber as shown in figure 5. The appropriate vertical load was applied to the rigidly locked wheel and photographs were taken at various braking-load values, including the unbraked condition. The deformations within the footprint were obtained from enlargements of these photographs.

Rolling Tests

The objectives of the braked- and unbraked-rolling tests were to measure the deformation or stretch within the footprint and to determine the braked and unbraked tire rolling radii. Two different test procedures were required to meet these objectives and each is described separately.

Deformation within the footprint.- The test procedure involved rolling the tire under the desired vertical load over the glass plate. The brake pressure was preset at values which were sufficient to develop the desired braking force but incapable of producing a locked-wheel skid. Tire deformation within the footprint resulting from the combined vertical load and braking force was determined from photographs taken through the glass plate in the same manner described for the static-loading tests.

Braked and unbraked tire rolling radii.- Figure 6 is a photograph of the carriage during tests to determine braked and unbraked tire rolling radii. The tests were conducted on a dry runway at the desired vertical loads and braking forces. Data were obtained at speeds of 5, 50, and 100 knots over distances in excess of 61 m (200 ft) and were recorded as time histories. Measurements of the vertical load and braking force were obtained from the instrumented dynamometer. The braked and unbraked tire rolling radii were calculated from measurements of the distance traveled along the runway and the angular displacements of the wheel.

RESULTS AND DISCUSSION

Fore-and-Aft Spring Constant

The fore-and-aft spring constant of a tire is a fundamental property which defines the overall elastic deformation of the tire in the braking mode. This property was obtained experimentally for each tire under two vertical loads by relating the applied braking force to the resulting overall footprint displacement.

Typical fore-and-aft force-deflection data for the tire footprint under static-loading conditions are presented in figure 7. These data were obtained over one and one-half loading cycles to establish a complete hysteresis loop. The fore-and-aft spring constant K_x was taken as the slope of the line which connected the end points of this loop. Spring constants computed for the two test tires, each under two vertical loads, are presented in table II. The table shows that the spring constant increases with increasing vertical load, the same trend noted in reference 6.

Static Response

The empirical expression of reference 9, which describes the elastic behavior of a tire during braking as determined from static measurements taken in the tire free-tread periphery, was based upon two fundamental assumptions. First, the expression assumed, on the basis of the trend defined by three data points from reference 8, that the displacement within the tire free-tread periphery varies exponentially with the peripheral distance from the leading edge of the footprint. The second fundamental assumption is that no additional deformation takes place within the footprint. The sections which follow discuss the results of tests to evaluate the validity of these assumptions.

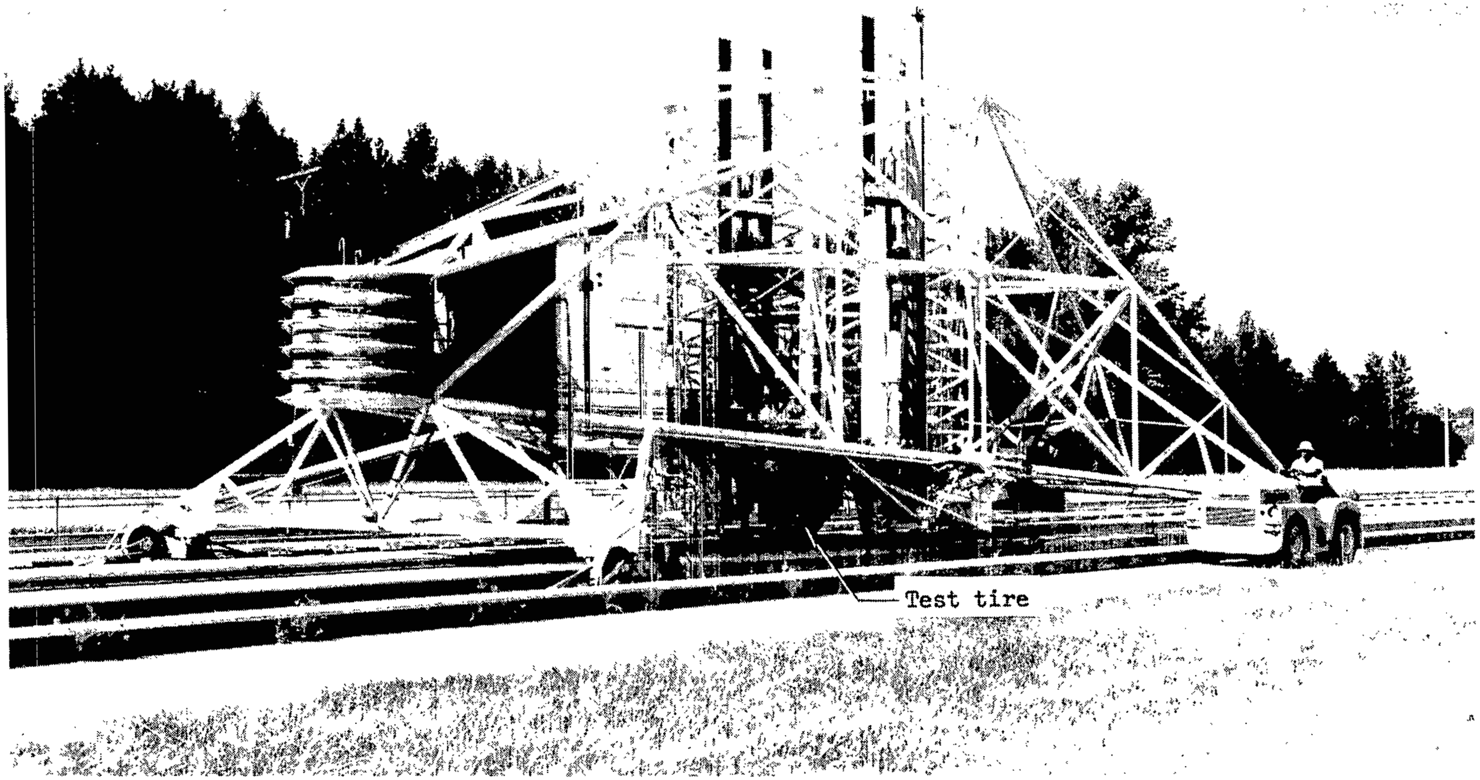

L-71-657

Figure 6.- Carriage and towing vehicle during low-speed braked-rolling tests.

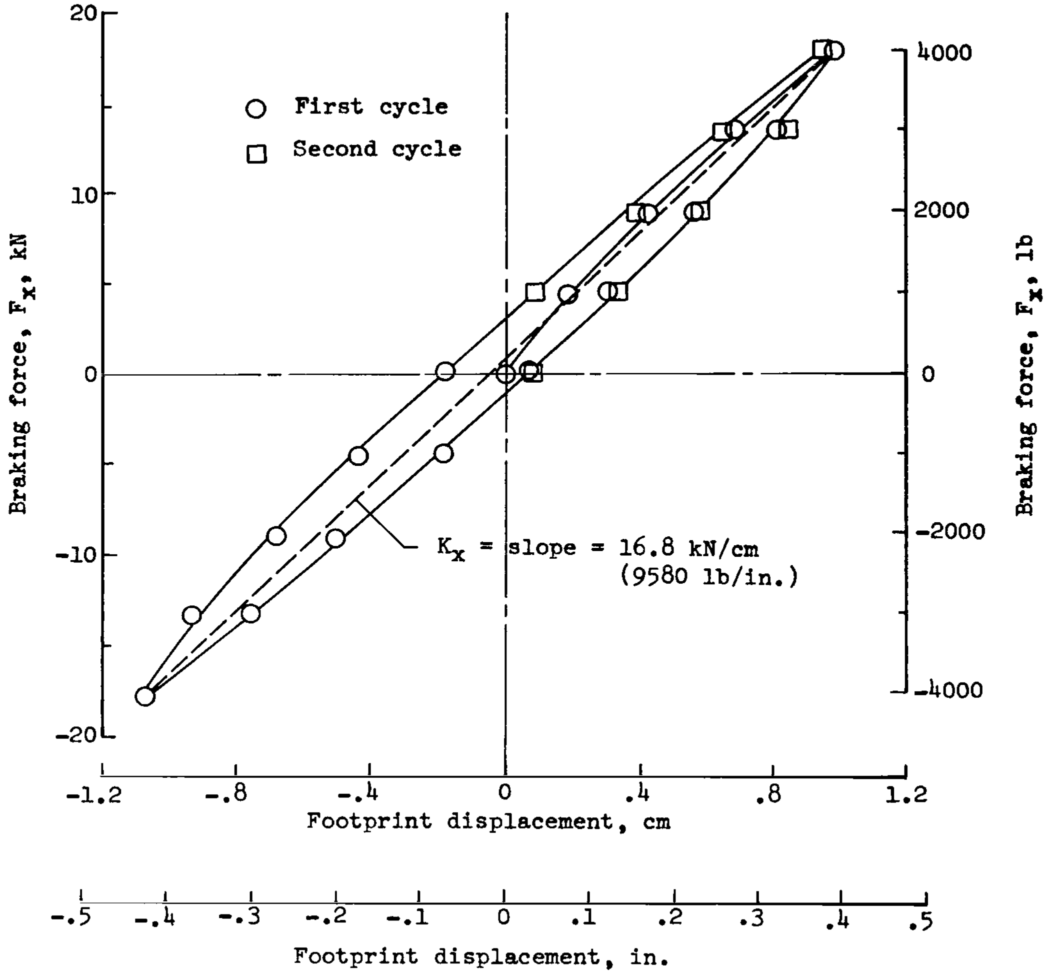

Figure 7.- Typical footprint fore-and-aft force-deflection curve. Tire A, F_z = 51.2 kN (11 500 lb).

TABLE II.- SUMMARY OF FORE-AND-AFT SPRING CONSTANTS FROM STATIC-LOADING TESTS

Tire	F_z		K_x	
	kN	lb	kN/cm	lb/in.
A	51.2	11 500	16.8	9 580
	98	22 000	22.7	12 900
B	107	24 000	20.0	11 400
	138	31 000	21.6	12 300

Displacement in the free-tread periphery.- Experimental tests were performed to investigate the variation of displacement within the tire free-tread periphery under static forces. An example of the results from these tests is presented in figure 8 where the displacement is plotted on a logarithmic scale as a function of the peripheral distance from the leading edge of the footprint plotted on a linear scale. As in reference 9, it is assumed that the maximum tire deformation occurs at the leading edge of the footprint; therefore during braking the displacement of this point from its unbraked position, identified as u_{p_o} in figure 1(b), is described by F_x/K_x. The displacement at other points along the free-tread periphery $\left(u_{p_i}\text{ in fig. 1(b)}\right)$ was obtained by subtracting from the maximum displacement the deformation accumulated between the leading edge of the

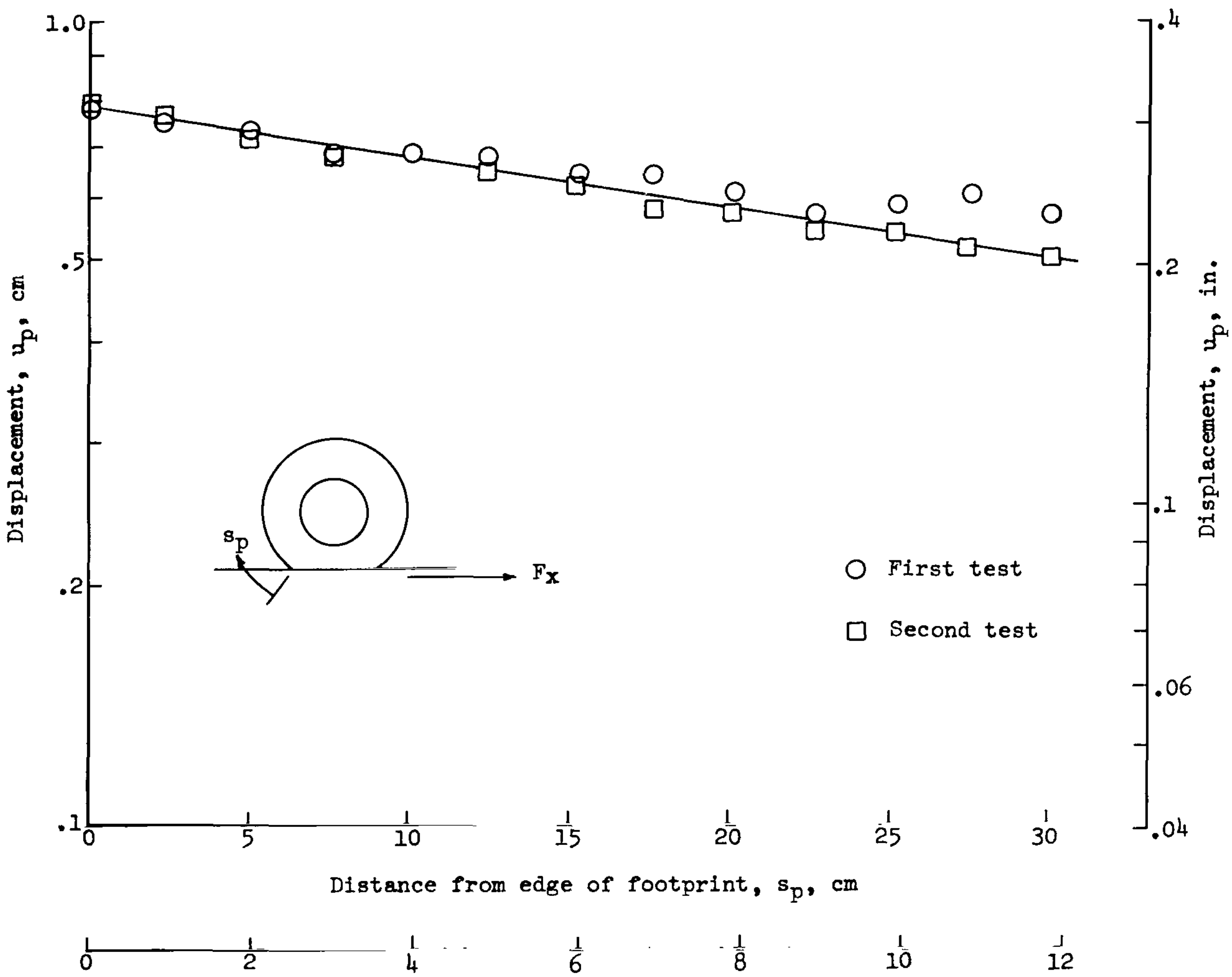

Figure 8.- Typical variation of displacements along tire free-tread periphery under static-loading conditions. Tire A, F_x = 13.35 kN (3000 lb); F_z = 51.2 kN (11 500 lb).

footprint and the point in question. The linearity of the data in this figure indicates that tire displacement varies exponentially with the distance from the leading edge of the footprint and, as such, validates the assumed displacement distribution necessary in the empirical analysis of reference 9. The data of figure 8 were obtained with tire A under a vertical loading of 51.2 kN (11 500 lb) and a braking force of 13.35 kN (3000 lb). Results from other loading conditions including those associated with tire B indicated a similar variation in tire displacement. The empirical expression which describes this variation is of the form

$$u_p = \frac{F_x}{K_x} e^{-s_p / J_{x,p}} \tag{1}$$

where $-1/J_{x,p}$ is the slope of the stretch curves typified by that of figure 8 and $J_{x,p}$ is referred to as the decay length and is a fundamental tire elastic parameter which defines the stretch distribution.

In an effort to extend the limited amount of available data which treat this parameter, the values of the decay lengths obtained from the various tests of this report are summarized and presented in figure 9. The figure shows that $J_{x,p}$ is essentially independent of the braking force and insensitive to variations in the vertical load over the range tested. These results indicate that $J_{x,p}$ is a constant associated with each tire and can be used in conjunction with the tire spring constant to define the elastic response of an aircraft tire to braking loads.

Deformation in the static footprint.- Experimental tests were performed to investigate the deformation within the static footprint resulting from braking forces. The results from these tests are presented in figure 10 for tires A and B where the displacements along the periphery are plotted as a function of the distance from the leading edge of the footprint. The displacement within each footprint due to braking corresponds to the change in distance from the leading edge of the footprint to preselected stations. Data are included in the figure for two vertical-loading conditions together with a simulated braking force which was applied to each wheel at levels comparable to those employed in other static tests of this study.

Since the displacements of figure 10 are accumulative from the leading edge of the footprint, positive slopes denote localized stretching and negative slopes denote localized relaxation. Thus, positive displacements define tension and negative displacements define compression. The figure shows that there is essentially no deformation in the footprints of tire A except for some stretching near the leading edge and some compression which appeared in the trailing portion of the footprints. Deformations at the leading edge are much more pronounced for tire B than for tire A. For the heavily loaded tire B, the stretching continues into the region near the center of the footprint. The nature of the deformations, particularly just beyond the leading portion of the footprint, suggests that localized adhesion is occurring in the tire-pavement interface for all but the heavily loaded tire B.

On the basis of the data of figure 10, it appears that the assumption of reference 9, regarding no stretching within the footprint, is not valid for all loading conditions. Thus, the empirical analysis of reference 9 does not adequately describe the response of all bias-ply aircraft tires to braking loads and a need exists to explore other means for defining the elastic behavior of a braked rolling tire.

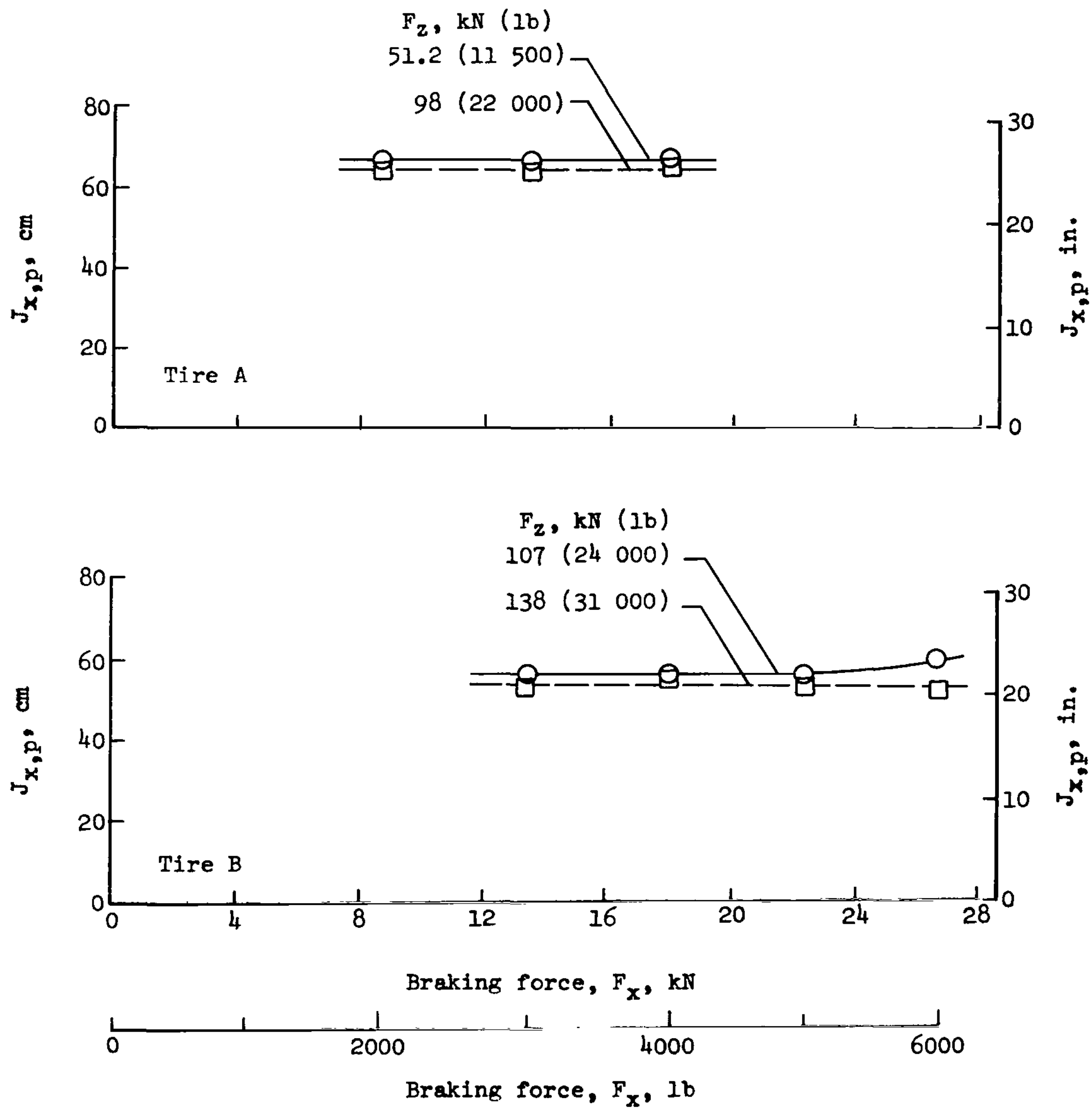

Figure 9.- Summary of decay lengths in free-tread periphery of test tires under various static-loading conditions.

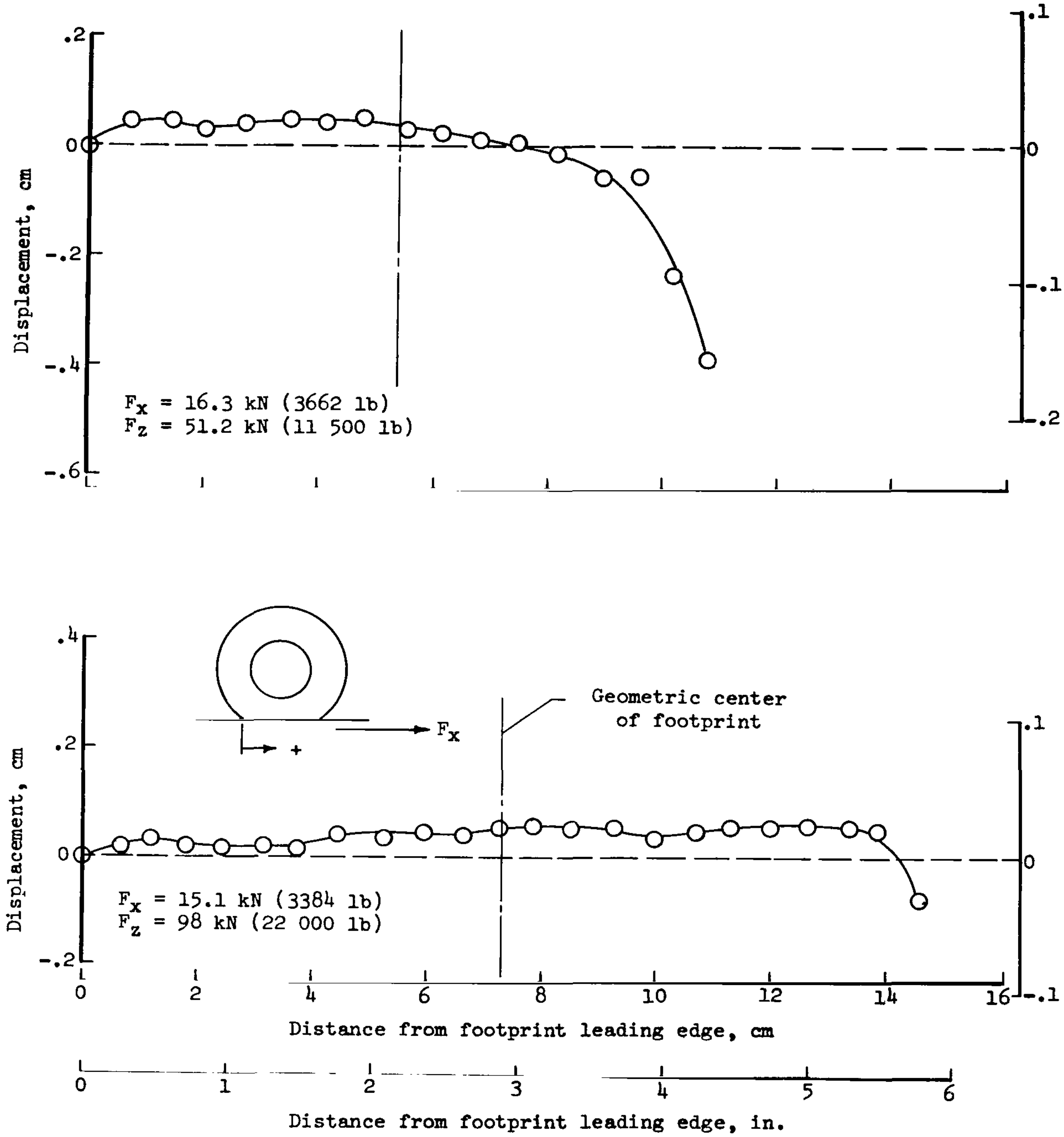

(a) Tire A.

Figure 10.- Displacement within footprint of test tires under static-loading conditions.

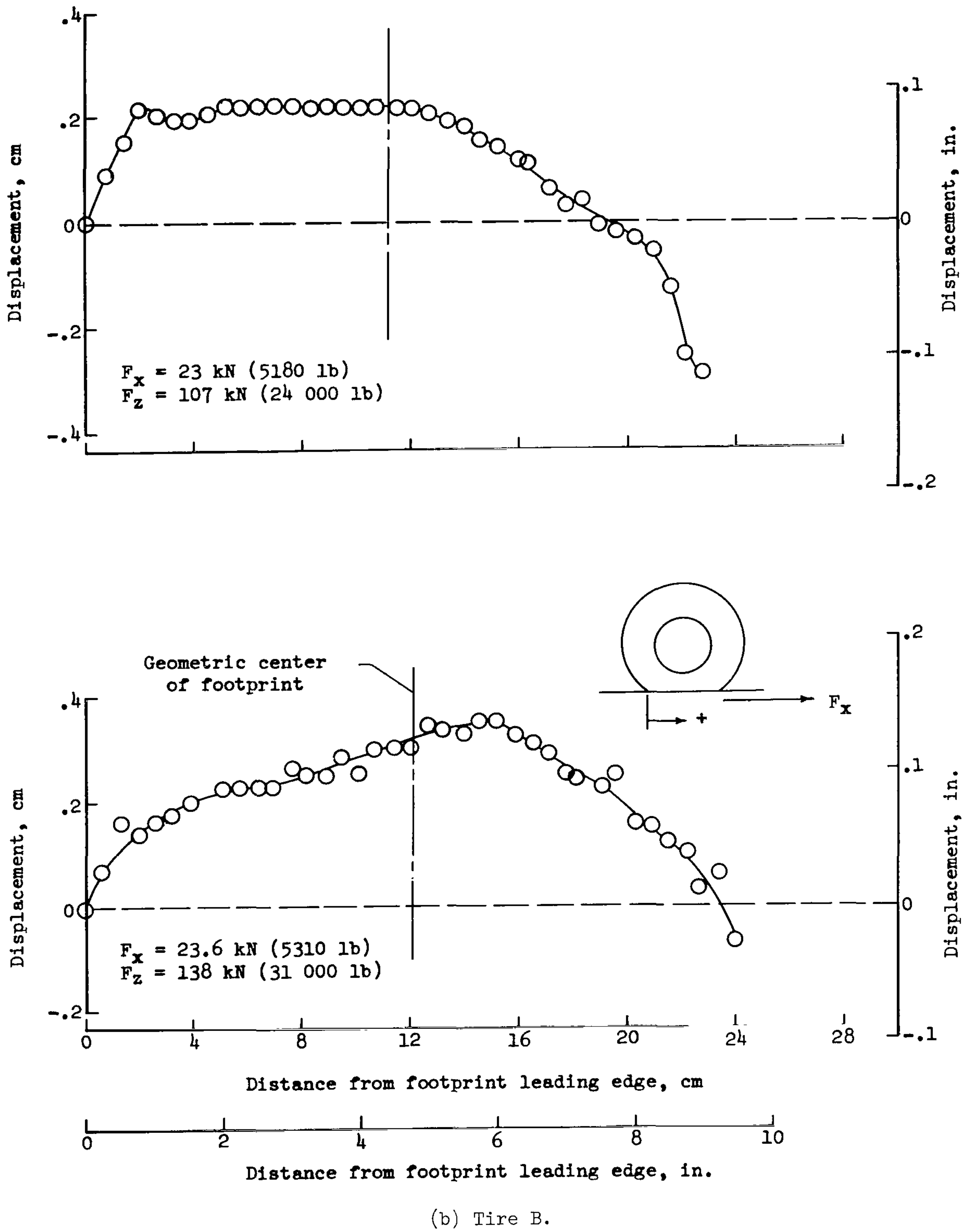

(b) Tire B.

Figure 10.- Concluded.

Braked-Rolling Response

The empirical analysis of reference 9 yields an approximation of the elastic response of the braked rolling tire based upon an equation which was developed from static deformation measurements in the free-tread periphery. This section presents the results of tests to develop an empirical expression for tire displacement from actual braked-rolling measurements.

Fore-and-aft peripheral displacements within the footprints of tires A and B during low-speed braked-rolling tests are presented in figure 11. Data are provided for loading conditions which were comparable to those used in the static tests. The displacement of the geometrical center of the footprint, which was observed to be the point of maximum tire deformation, was set equal to F_x/K_x. The displacements at other points within the footprint were obtained by subtracting the deformation accumulated from the center of the footprint to the point in question. Values of the spring constant K_x for each tire were obtained from the static measurements listed in table II. The figure indicates that stretching occurs in the region from the leading edge to the center of the braked-rolling footprint (negative slope) while relaxation occurs in the region from the center of the footprint to the trailing edge (positive slope). The smooth variation of the stretch noted in the figure indicates the absence of localized adhesion within the tire-pavement interface under braked-rolling conditions and suggests that the tire displacement within the footprint can be defined by a simple mathematical expression. To this end the displacements within the leading half of the footprints were plotted on a logarithmic scale as a function of the distance from the center of the footprint on a linear scale in figure 12. The figure shows that the displacements for each test condition vary exponentially with distance from the center of the footprint and lead to the following expression:

$$u_f = \frac{F_x}{K_x} e^{-s_f/J_{x,f}} \tag{2}$$

where $-1/J_{x,f}$ is the slope of the curves in figure 11 and $J_{x,f}$ is the characteristic length in the braked-rolling footprint which corresponds to the peripheral decay length of the free-tread periphery. Table III lists the values of $J_{x,f}$ for the different braked-rolling test conditions and also includes the corresponding values of $J_{x,p}$ obtained from the faired data of figure 9. The data show that the magnitude of corresponding J_x values for tire B are similar but indicate that $J_{x,f}$ is higher than $J_{x,p}$ for each corresponding tire-A test condition.

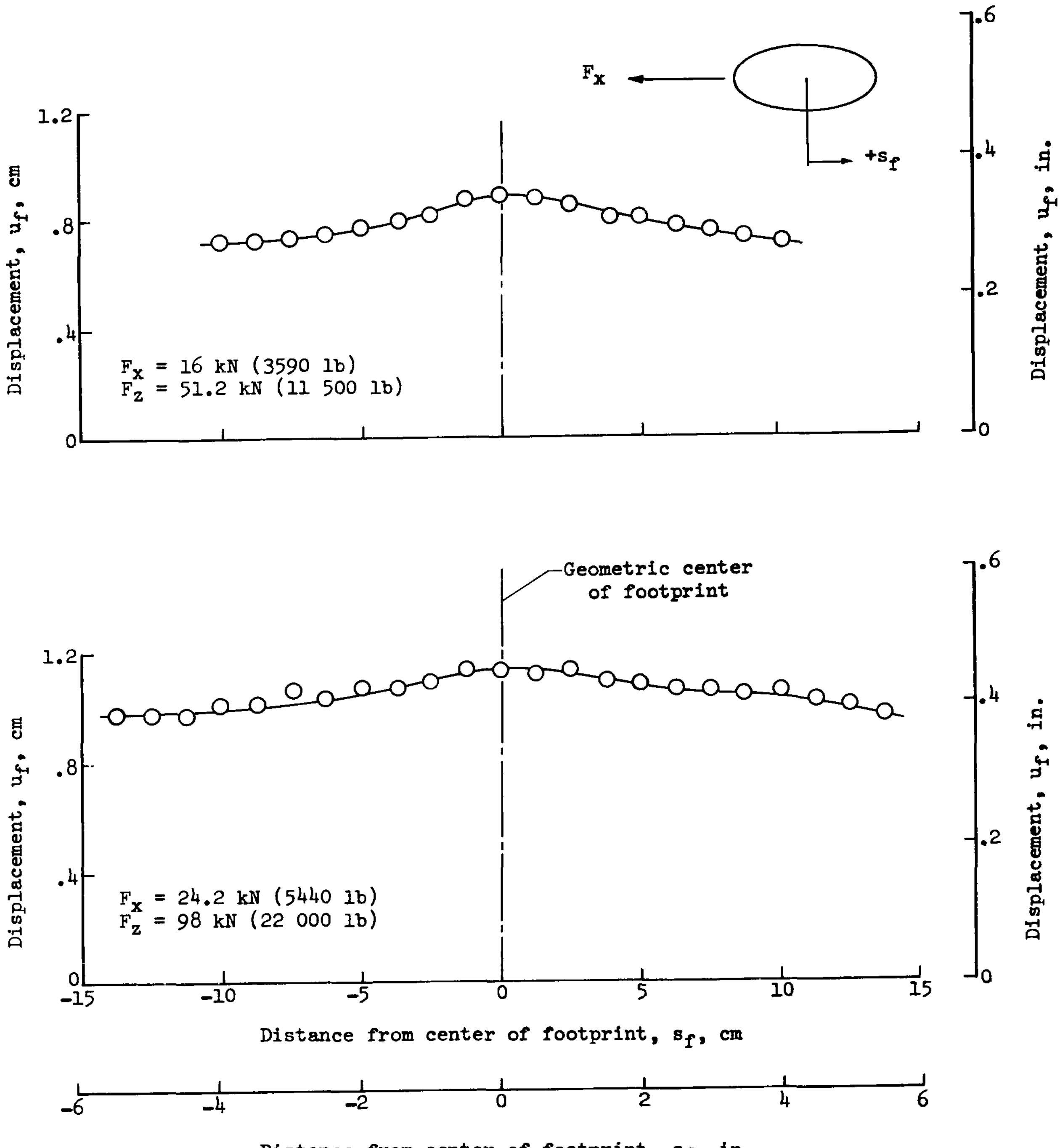

(a) Tire A.

Figure 11.- Displacement within footprints of braked rolling tires.

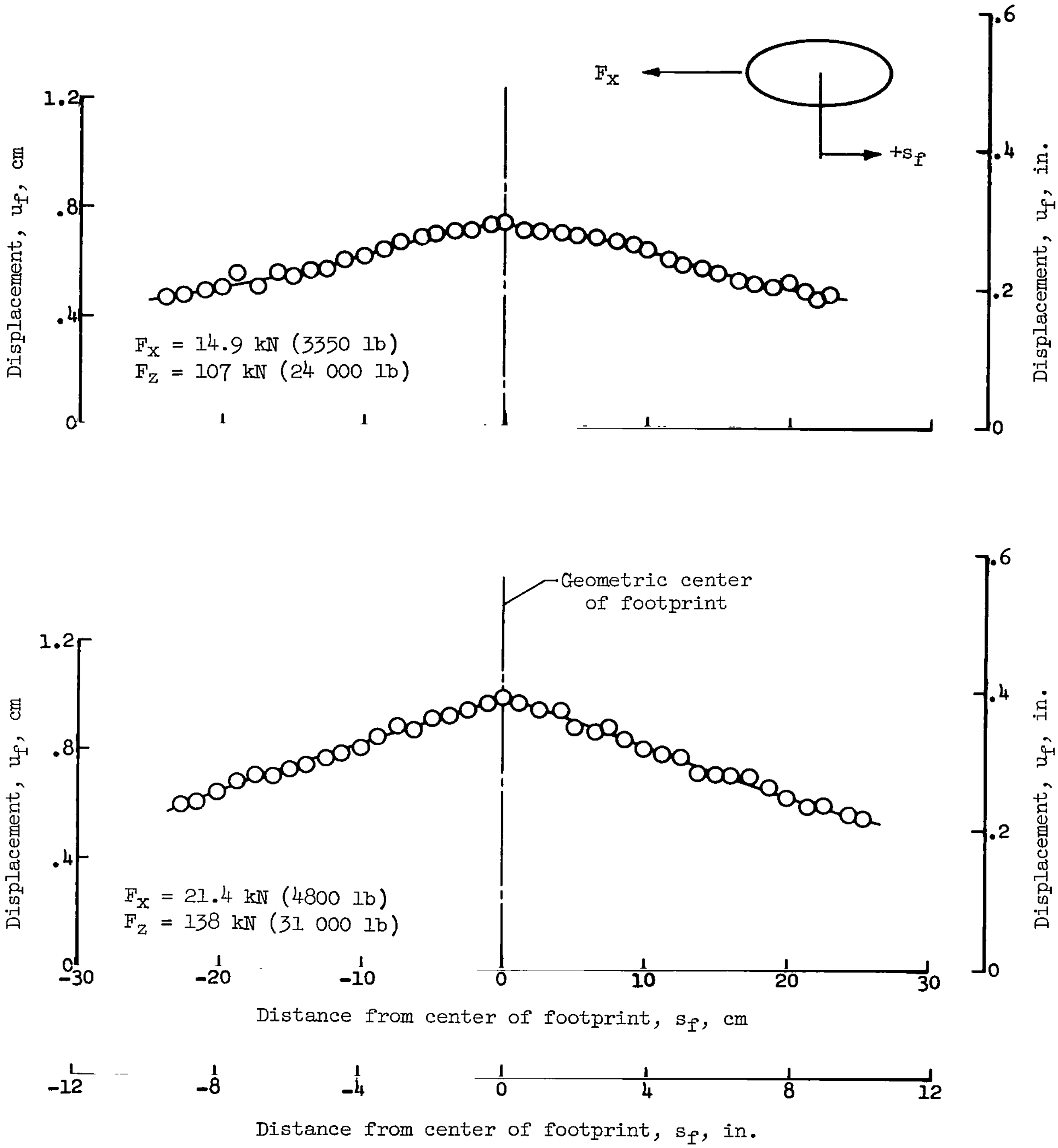

(b) Tire B.

Figure 11.- Concluded.

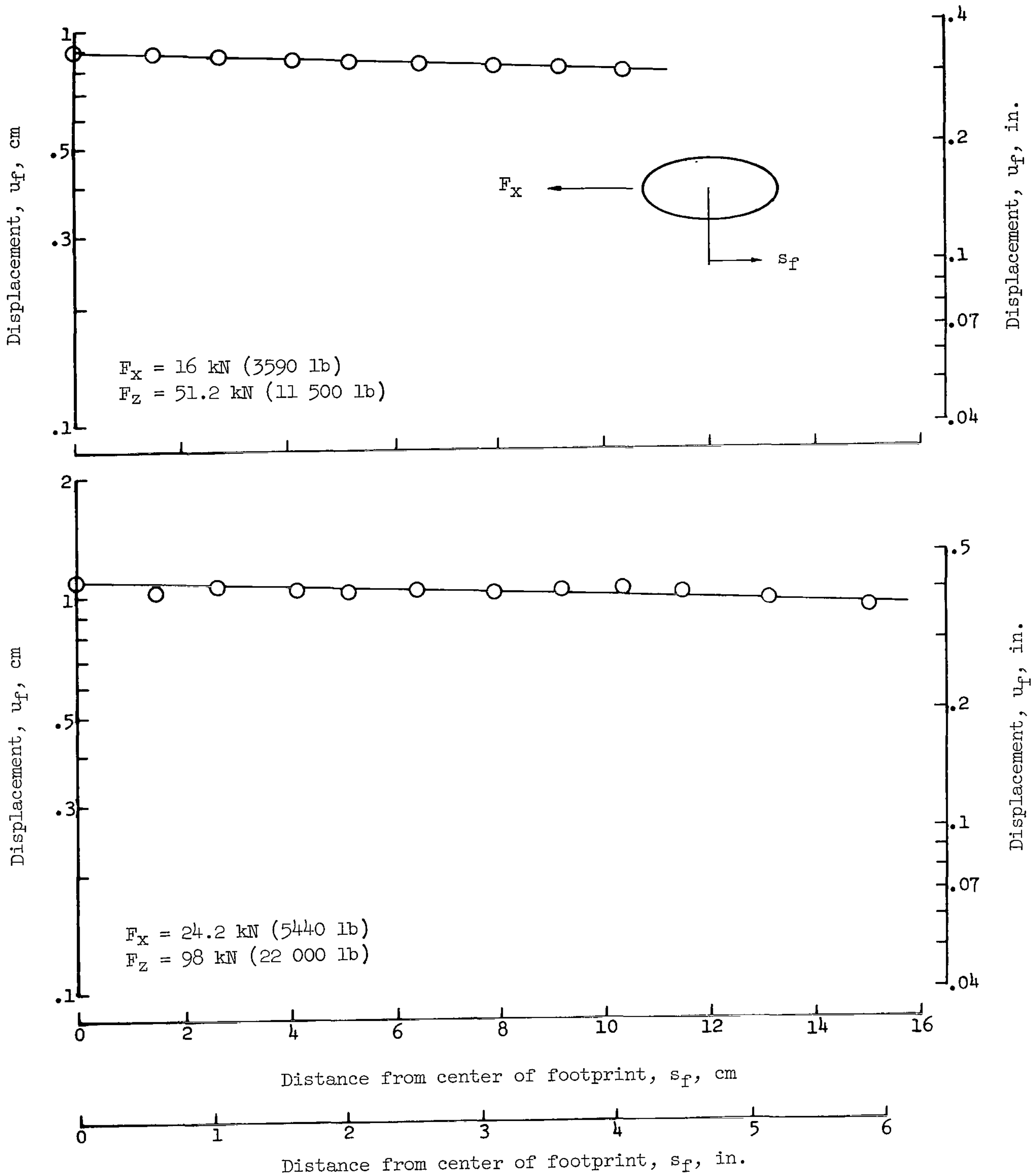

(a) Tire A.

Figure 12.- Variation of displacement within footprint of braked rolling tires.

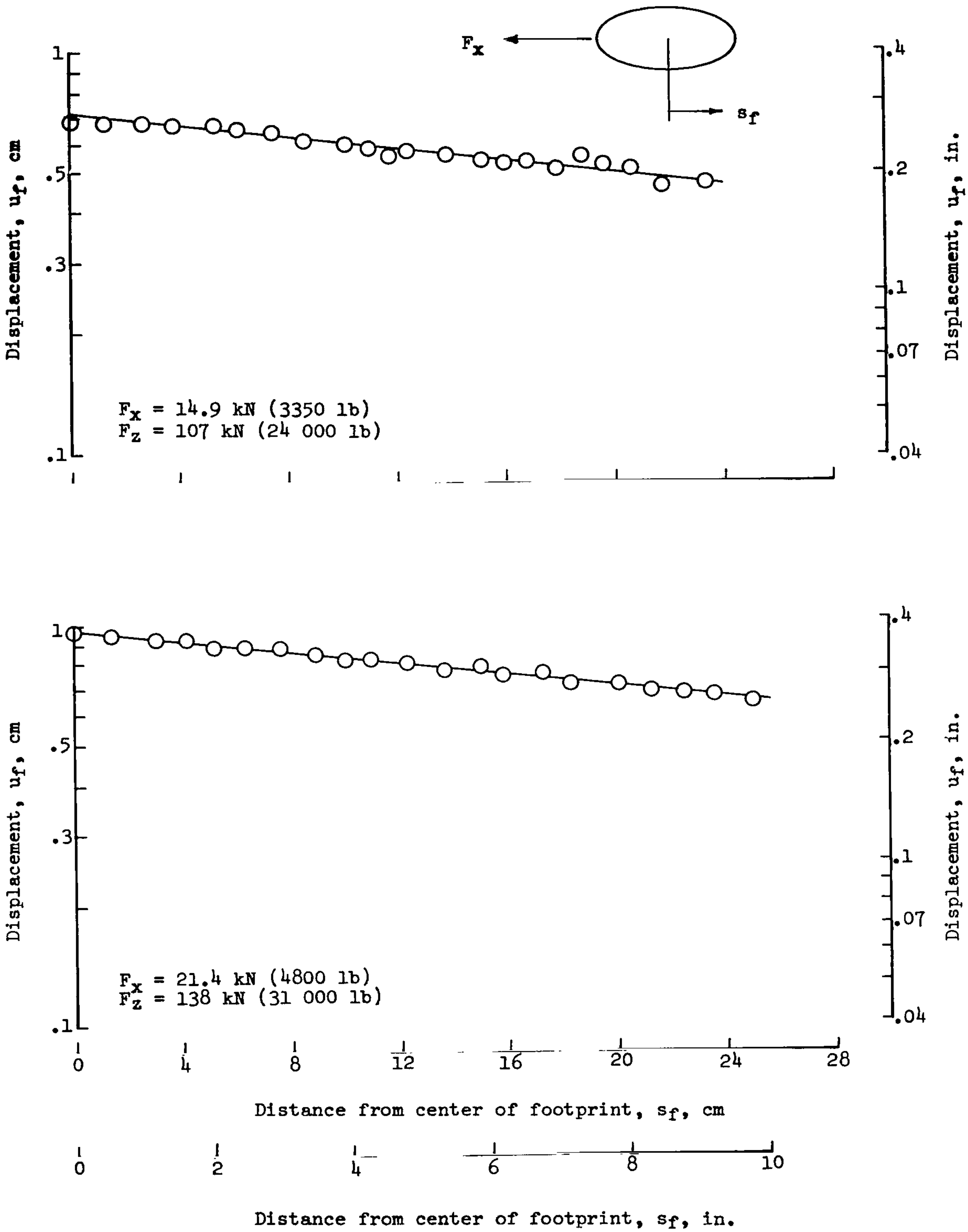

(b) Tire B.

Figure 12.- Concluded.

TABLE III.- SUMMARY OF DECAY LENGTHS COMPUTED FROM STATIC-LOADING AND BRAKED-ROLLING TESTS

Tire	F_z		F_x		$J_{x,f}$		$J_{x,p}$	
	kN	lb	kN	lb	cm	in.	cm (a)	in. (a)
A	51.2	11 500	16.0	3590	71.1	28.0	66.5	26.2
	98	22 000	24.2	5440	84.5	33.3	64.5	25.4
B	107	24 000	14.9	3350	50.8	20	55.9	22.0
	138	31 000	21.4	4800	55.9	22	53.4	21.0

[a]From faired data of figure 9.

Application of Results

The fore-and-aft elastic behavior of a tire may be reflected in changes to the rolling radius attributed to braking. The expression for the change in rolling radius Δr is developed in the appendix. This expression is based upon the empirical equations which describe tire displacement within both the braked-rolling footprint and the free-tread periphery under static-loading conditions. This change is given by the general expression

$$\Delta r = \frac{rF_x}{J_x K_x} \tag{3}$$

Experimental braked- and unbraked-rolling tests were conducted to evaluate the ability of equation (3) to predict changes in the rolling radii of the two test tires under various loading conditions. Values of Δr presented in table IV were obtained experimentally from low-speed tests with tire A and from tests with tire B at ground speeds up to 100 knots.

The experimental change in rolling radius Δr_{exp} is the difference between the rolling radii of the braked and the freely rotating tire, determined in each case by relating the distance traveled to the number of tire revolutions. The calculated values of Δr_p and Δr_f also presented in table IV are based upon equation (3) using values of $J_{x,p}$ obtained under static-loading conditions (ref. 9) and $J_{x,f}$ obtained under low-speed braked-rolling conditions, respectively. For the purpose of these calculations $J_{x,f}$ was assumed to be independent of the braking force as was observed in the free-tread-periphery measurements. With this assumption, the change in rolling radius is directly proportional to the braking force. The changes in rolling radius during braking as calculated from both static and braked- and unbraked-rolling tests are compared in figure 13

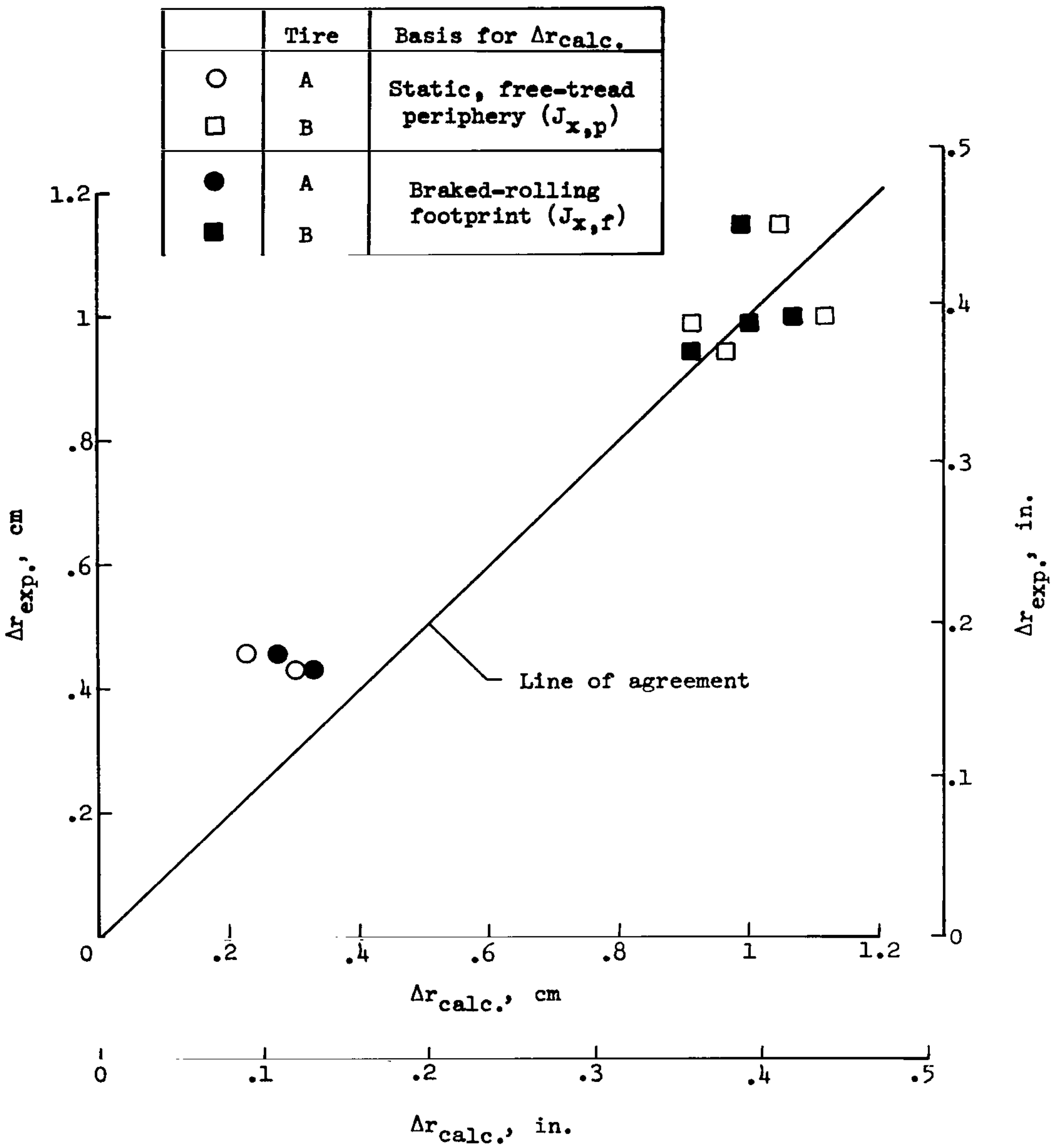

Figure 13.- Comparison of experimental and calculated change in rolling radius attributed to braking.

TABLE IV.- SUMMARY OF BRAKED AND UNBRAKED

TIRE ROLLING RADIUS MEASUREMENTS

Tire	Ground speed, knots	F_z		F_x		$r_{o,exp}$		$r_{e,exp}$		Δr_{exp}		Δr_p		Δr_f	
		kN	lb	kN	lb	cm	in.	cm	in.	cm	in.	cm	in.	cm	in.
A	5	51.2	11 500	9.85	2190	36.47	14.36	36.91	14.53	0.44	0.17	0.30	0.12	0.33	0.13
	5	98	22 000	11.5	2590	35.79	14.09	36.25	14.27	.46	.18	.23	.09	.28	.11
B	5	107	24 000	16.6	3730	58.78	23.14	59.77	23.53	0.99	0.39	0.92	0.36	1.02	0.40
	5	138	31 000	18.1	4057	58.27	22.94	59.21	23.31	.94	.37	.97	.38	.92	.36
	50	138	31 000	20.6	4630	58.42	23.00	59.44	23.40	1.02	.40	1.12	.44	1.07	.42
	100	138	31 000	19.4	4370	59.06	23.25	60.20	23.70	1.14	.45	1.05	.41	.99	.39

with those obtained experimentally. The figure shows reasonably good agreement between the calculated and experimental data. The empirical expression for calculating Δr was developed solely from the tire elastic behavior and assumes no slippage. The small differences between the calculated values of Δr for both tires (see fig. 13) are the result of differences in the corresponding decay lengths presented in table III.

The data of figure 13 suggest that the change in rolling radius due to braking can be predicted with reasonable accuracy from elastic measurements of the static free-tread periphery or from elastic measurements within the footprint during low-speed braking. Furthermore, since changes in the rolling radius as calculated on the basis of tire deformations alone are comparable to those measured experimentally, what was heretofore considered as pure tire slippage under braked-rolling conditions (in the stable region of the braking-friction—slip curve) may be wholly or in part the result of tire elasticity. Thus, the elastic behavior of a tire results in apparent slip ratios which are not precisely related to the friction developed in the tire-pavement interface. This elastic behavior, therefore, must be considered in the design or application of efficient automatic braking systems.

CONCLUDING REMARKS

A study was made at Langley Research Center to evaluate the elastic behavior of a braked rolling tire and to relate this behavior to the characteristics of the tire as obtained from simple static flexure tests. The study consisted of static and braked- and unbraked-rolling tests of two types of bias-ply aircraft tires and an analysis which related tire reaction to the braking forces.

The results of this investigation indicate that the decay length is a constant associated with each tire and can be used in conjunction with the spring constant to define the elastic response of an aircraft tire to braking forces. It has been demonstrated that changes in the rolling radius due to braking can be predicted with reasonable accuracy from elastic measurements of the static free-tread periphery or from elastic measurements within the footprint during low-speed braking, assuming no slippage between the tire and the pavement. Furthermore, since changes in the rolling radius as calculated on the basis of tire deformations alone are comparable to those measured experimentally, what was heretofore considered as pure tire slippage under braked-rolling conditions may be wholly or in part the result of tire elasticity. Therefore, the elastic behavior of a tire must be considered in the design or application of efficient automatic braking systems.

Langley Research Center,
National Aeronautics and Space Administration,
Hampton, Va., July 16, 1971.

APPENDIX

ANALYSIS

This appendix develops the expression which relates tire elasticity to changes in the rolling radius attributed to braking. The analysis is similar to that of reference 9 applied to treat the displacement which occurs in the leading half of the braked-rolling footprint. The assumptions used in the analysis are as follows:

1. There is no relative motion between the tire and the ground at the geometric center of the footprint.

2. The spring constant K_x determined from static measurements is independent of forward speed.

The braked tire rolling radius r_e of an aircraft tire is defined by the following expression:

$$r_e = r\left(1 + \epsilon_z + \epsilon_{x,max}\right) \tag{A1}$$

where ϵ_z is the strain caused by vertical loading and $\epsilon_{x,max}$ is the maximum strain resulting from the braking force.

The unbraked tire rolling radius is similarly defined as

$$r_o = r\left(1 + \epsilon_z\right) \tag{A2}$$

Substituting equation (A2) into (A1) yields

$$r_e = r_o + r\epsilon_{x,max} \tag{A3}$$

and the change in rolling radius is defined as

$$\Delta r = r_e - r_o = r\epsilon_{x,max} \tag{A4}$$

Data from the braked-rolling tests indicate that tire displacement can be expressed as

$$u_f = \frac{F_x}{K_x} e^{-s_f/J_{x,f}} \tag{A5}$$

The unit elongation strain is thus

$$\epsilon_x = -\frac{d(u_f)}{ds_f} = \frac{F_x}{J_{x,f}K_x} e^{-s_f/J_{x,f}} \tag{A6}$$

The negative sign on the differentiation in equation (A6) is necessary because the tire displacement decreases as the distance from the center of the footprint increases.

Since the rolling radius is related to the maximum elongation strain equation (A6) is evaluated at $s_f = 0$ to yield

$$\epsilon_{x,max} = \epsilon_x \Big|_{s_f=0} = \frac{F_x}{J_{x,f}K_x} \tag{A7}$$

and the expression for change in the rolling radius is

$$\Delta r = r_e - r_o = \frac{rF_x}{J_{x,f}K_x} \tag{A8}$$

This expression is identical to that of reference 9 developed from stretching in the free-tread periphery of a statically loaded tire where $J_{x,p}$ corresponds to $J_{x,f}$.

REFERENCES

1. Bourcier De Carbon, Christian: Analytical Study of Shimmy of Airplane Wheels. NACA TM 1337, 1952.
2. Schlippe, B.; and Dietrich, R.: Shimmying of a Pneumatic Wheel. Papers on Shimmy and Rolling Behavior of Landing Gears Presented at Stuttgart Conference Oct. 16 and 17, 1941, NASA TM 1365, 1954, pp. 125-160, 217-228.
3. Hadekel, R.: The Mechanical Characteristics of Pneumatic Tyres – A Digest of Present Knowledge. S & T Memo. No. 10/52, TPA 3/TIB, Brit. Min. Supply, Nov. 1952.
4. Horne, Walter B.; and Smiley, Robert F.: Low-Speed Yawed-Rolling Characteristics and Other Elastic Properties of a Pair of 40-Inch-Diameter, 14-Ply-Rating, Type VII Aircraft Tires. NACA TN 4109, 1958.
5. Schuster, Robert; and Weichsler, Paul: Der Kraftschluss zwischen Rad und Fahrbahn. Automobiltechnische Z., Jahrgang 38, Heft 20, Oct. 25, 1935, pp. 499-504.
6. Horne, Walter B.: Static Force-Deflection Characteristics of Six Aircraft Tires Under Combined Loading. NACA TN 2926, 1953.
7. Dodge, R. N.; Orne, David; and Clark, S. K.: Fore-and-Aft Stiffness Characteristics of Pneumatic Tires. NASA CR-900, 1967.
8. Boeckh: Ermittlung der elastischen Konstanten von Flugzeugreifen (Determination of the Elastic Constants of Airplane Tires). Focke-Wulf Flugzeugbau G.m.b.H. (Bremen), Dec. 1944. (Available in English translation as NACA TM 1378.)
9. Smiley, Robert F.; and Horne, Walter B.: Mechanical Properties of Pneumatic Tires With Special Reference to Modern Aircraft Tires. NASA TR R-64, 1960. (Supersedes NACA TN 4110.)
10. Batterson, Sidney A.: A Study of the Dynamics of Airplane Braking Systems as Affected by Tire Elasticity and Brake Response. NASA TN D-3081, 1965.
11. Horne, Walter B.; and Leland, Trafford J. W.: Influence of Tire Tread Pattern and Runway Surface Condition on Braking Friction and Rolling Resistance of a Modern Aircraft Tire. NASA TN D-1376, 1962.
12. Joyner, Upshur T.; Horne, Walter B.; and Leland, Trafford J. W.: Investigation of the Ground Performance of Aircraft Relating to Wet Runway Braking and Slush Drag. AGARD Rep. 429, Jan. 1963.

NASA-Langley, 1971 —— 2 L-6605

NATIONAL AERONAUTICS AND SPACE ADMINISTRATION
WASHINGTON, D.C. 20546

OFFICIAL BUSINESS
PENALTY FOR PRIVATE USE $300

FIRST CLASS MAIL

POSTAGE AND FEES PAID
NATIONAL AERONAUTICS AND
SPACE ADMINISTRATION

020 001 C1 U 02 710910 S00903DS
DEPT OF THE AIR FORCE
AF SYSTEMS COMMAND
AF WEAPONS LAB (WLOL)
ATTN: E LOU BOWMAN, CHIEF TECH LIBRARY
KIRTLAND AFB NM 87117

POSTMASTER: If Undeliverable (Section 158 Postal Manual) Do Not Return

"The aeronautical and space activities of the United States shall be conducted so as to contribute . . . to the expansion of human knowledge of phenomena in the atmosphere and space. The Administration shall provide for the widest practicable and appropriate dissemination of information concerning its activities and the results thereof."

— NATIONAL AERONAUTICS AND SPACE ACT OF 1958

NASA SCIENTIFIC AND TECHNICAL PUBLICATIONS

TECHNICAL REPORTS: Scientific and technical information considered important, complete, and a lasting contribution to existing knowledge.

TECHNICAL NOTES: Information less broad in scope but nevertheless of importance as a contribution to existing knowledge.

TECHNICAL MEMORANDUMS: Information receiving limited distribution because of preliminary data, security classification, or other reasons.

CONTRACTOR REPORTS: Scientific and technical information generated under a NASA contract or grant and considered an important contribution to existing knowledge.

TECHNICAL TRANSLATIONS: Information published in a foreign language considered to merit NASA distribution in English.

SPECIAL PUBLICATIONS: Information derived from or of value to NASA activities. Publications include conference proceedings, monographs, data compilations, handbooks, sourcebooks, and special bibliographies.

TECHNOLOGY UTILIZATION PUBLICATIONS: Information on technology used by NASA that may be of particular interest in commercial and other non-aerospace applications. Publications include Tech Briefs, Technology Utilization Reports and Technology Surveys.

Details on the availability of these publications may be obtained from:

SCIENTIFIC AND TECHNICAL INFORMATION OFFICE

NATIONAL AERONAUTICS AND SPACE ADMINISTRATION

Washington, D.C. 20546